J|A|C|S ARTICLES

Published on Web 09/07/2010

Folding Catalysis by Transient Coordination of Zn^{2+} to the Cu Ligands of the ALS-Associated Enzyme Cu/Zn Superoxide Dismutase 1

Lina Leinartaitė,[†] Kadhirvel Saraboji,[‡] Anna Nordlund,[†] Derek T. Logan,[‡] and Mikael Oliveberg*,[†]

Department of Biochemistry and Biophysics, Arrhenius Laboratories of Natural Sciences, Stockholm University, S-106 91 Stockholm, Sweden, and Department of Biochemistry and Structural Biology, Lund University, S-221 00 Lund, Sweden

Received June 29, 2010; E-mail: mikael.oliveberg@dbb.su.se

Abstract: How coordination of metal ions modulates protein structures is not only important for elucidating biological function but has also emerged as a key determinant in protein turnover and protein-misfolding diseases. In this study, we show that the coordination of Zn^{2+} to the ALS-associated enzyme Cu/Zn superoxide dismutase (SOD1) is directly controlled by the protein's folding pathway. Zn^{2+} first catalyzes the folding reaction by coordinating transiently to the Cu ligands of SOD1, which are all contained within the folding nucleus. Then, after the global folding transition has commenced, the Zn^{2+} ion transfers to the higher affinity Zn site, which structures only very late in the folding process. Here it remains dynamically coordinated with an off rate of $\sim 10^{-5}$ s^{-1}. This relatively rapid equilibration of metals in and out of the SOD1 structure provides a simple explanation for how the exceptionally long lifetime, >100 years, of holoSOD1 is still compatible with cellular turnover: if a dissociated Zn^{2+} ion is prevented from rebinding to the SOD1 structure then the lifetime of the protein is reduced to a just a few hours.

Introduction

The radical scavenger Cu/Zn superoxide dismutase (SOD1) coordinates two metal ions: a redox-active $Cu^{2+/1+}$ that binds directly to the protein's central β-sheet scaffold and an adjacent Zn^{2+} that supports the structure of the long, functional loops encasing the active site (Figure 1). Besides orchestrating enzymatic function, the SOD1 metals are critical for maintaining the SOD1 molecule's stability and structural integrity:[1−5] loss of metal ions not only promotes SOD1 aggregation in vitro but also seems to trigger misfolding and "gain of toxic function" in the neurodegenerative disease *amyotrophic lateral sclerosis* (ALS). Of particular interest is here the role of the structural Zn^{2+} ion.[4−9] However, a caveat to studies of the metalated protein is that the Zn^{2+} ions coordinate with high affinity to both the Cu and Zn sites,[3,10] making the identity of the species at hand uncertain in some cases. To eliminate this problem, we have in previous work removed the Zn ligands by mutation to see how Zn^{2+} loss affects folding and stability of the SOD1 monomer.[3] As a result, the remaining Cu site ligands were found to coordinate their metal ion, either Cu^{2+} or Zn^{2+}, early in the folding process, causing a pronounced acceleration of the refolding kinetics.[3] This is because the Cu site ligands are contained within the folding nucleus of the SOD1 barrel. Even so, without the structural support of a metalated Zn site, one of the Cu site ligands (H48) fails to coordinate the metal ion, preventing ordering of the second coordination sphere in the folded state:[3] both loops IV and VII become disordered in the crystal structure (Figure 2), and the molecules cross-bind in the crystal lattice in a way that has been observed for several ALS-associated SOD1 mutations.[3,11] One role of the Zn site is thus to prevent SOD1 misfolding by keeping the loops such that correct Cu coordination can occur.[3]

In the present study, we complete the above picture by investigating the structural, kinetic, and thermodynamic effects of removing the SOD1 Cu site. The results show that, in contrast to the Cu site, the Zn site forms and coordinates its metal ion late in folding, and it does so without effect on the refolding rate constant. This temporal separation of Cu and Zn site formation along the folding coordinate leads to curious effects

[†] Stockholm University.
[‡] Lund University.

(1) Lynch, S. M.; Boswell, S. A.; Colon, W. *Biochemistry* **2004**, *43* (51), 16525–165231.
(2) Lynch, S. M.; Colon, W. *Biochem. Biophys. Res. Commun.* **2006**, *340* (2), 457–461.
(3) Nordlund, A.; Leinartaite, L.; Saraboji, K.; Aisenbrey, C.; Grobner, G.; Zetterstrom, P.; Danielsson, J.; Logan, D. T.; Oliveberg, M. *Proc. Natl. Acad. Sci. U.S.A.* **2009**, *106* (24), 9667–9672.
(4) Kayatekin, C.; Zitzewitz, J. A.; Matthews, C. R. *J. Mol. Biol.* **2008**, *384* (2), 540–5655.
(5) Rumfeldt, J. A.; Lepock, J. R.; Meiering, E. M. *J. Mol. Biol.* **2009**, *385* (1), 278–298.
(6) Crow, J. P.; Sampson, J. B.; Zhuang, Y.; Thompson, J. A.; Beckman, J. S. *J. Neurochem.* **1997**, *69* (5), 1936–1944.
(7) Kim, J.; Kim, T. Y.; Hwang, J. J.; Lee, J. Y.; Shin, J. H.; Gwag, B. J.; Koh, J. Y. *Neurobiol. Dis.* **2009**, *34* (2), 221–229.
(8) Puttaparthi, K.; Gitomer, W. L.; Krishnan, U.; Son, M.; Rajendran, B.; Elliott, J. L. *J. Neurosci.* **2002**, *22* (20), 8790–8796.
(9) Smith, A. P.; Lee, N. M. *Amyotrophic Lateral Scler.* **2007**, *8* (3), 131–143.
(10) Hirose, J.; Yamada, M.; Hayakawa, C.; Nagao, H.; Noji, M.; Kidani, Y. *Biochem. Int.* **1984**, *8* (3), 401–408.
(11) Elam, J. S.; Taylor, A. B.; Strange, R.; Antonyuk, S.; Doucette, P. A.; Rodriguez, J. A.; Hasnain, S. S.; Hayward, L. J.; Valentine, J. S.; Yeates, T. O.; Hart, P. J. *Nat. Struct. Biol.* **2003**, *10* (6), 461–467.

 © 2010 American Chemical Society

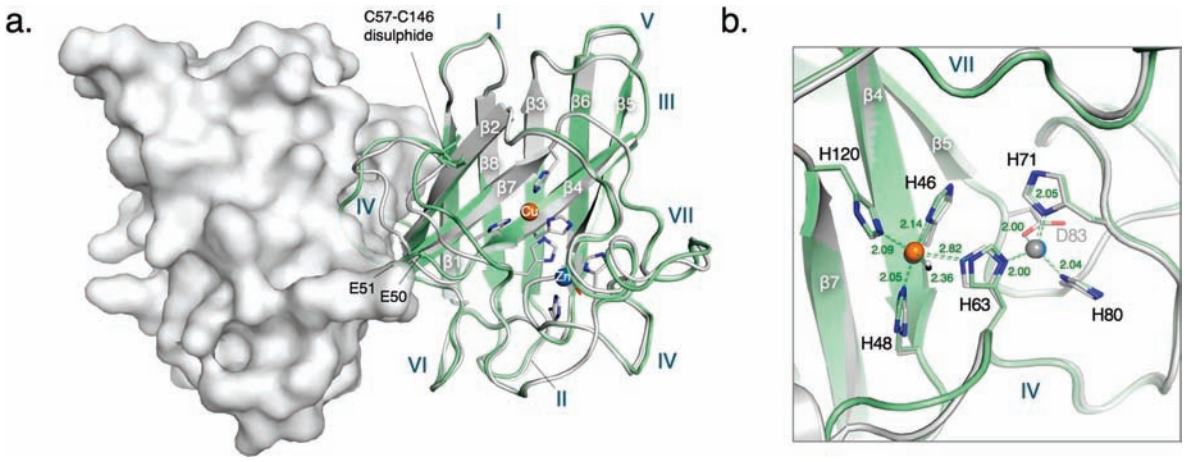

Figure 1. Structural features of the native SOD1 dimer (PDB entry 1HL5) and its monomeric variant holoSOD1^{CuZn} (this work). Each SOD1 monomer consists of 153 amino acids folded into an eight-stranded Greek key β-barrel with seven loops. The Cu and Zn ions of the active site are shown as orange and blue spheres, respectively. (a) Superposition of holoSOD1^{CuZn} (green) on one monomer of dimeric SOD1 (gray). The structure of the holoSOD1^{CuZn} monomer is overall similar to the monomers of native SOD1 dimer except for loop IV, which forms part of the dimer interface. The positions of the dimer-splitting mutations F50E/G51E are indicated as small spheres. (b) Close-up of the active site showing identical metal coordination in the holoSOD1^{CuZn} monomer and the native SOD1 dimer. Cu^{2+} is coordinated to H46, H48, H63, and H120 and a water molecule in a distorted square pyramidal geometry, whereas Zn^{2+} is coordinated to H63, H71, H80, and D83 in a distorted tetrahedral geometry. H63 acts as a bridge by coordinating both metals. Metal coordinated water molecules in holoSOD1^{CuZn} and the native SOD1 dimer are shown as white and black, respectively. Correspondingly, the metal−ligand interactions are indicated as green and gray dotted lines, respectively.

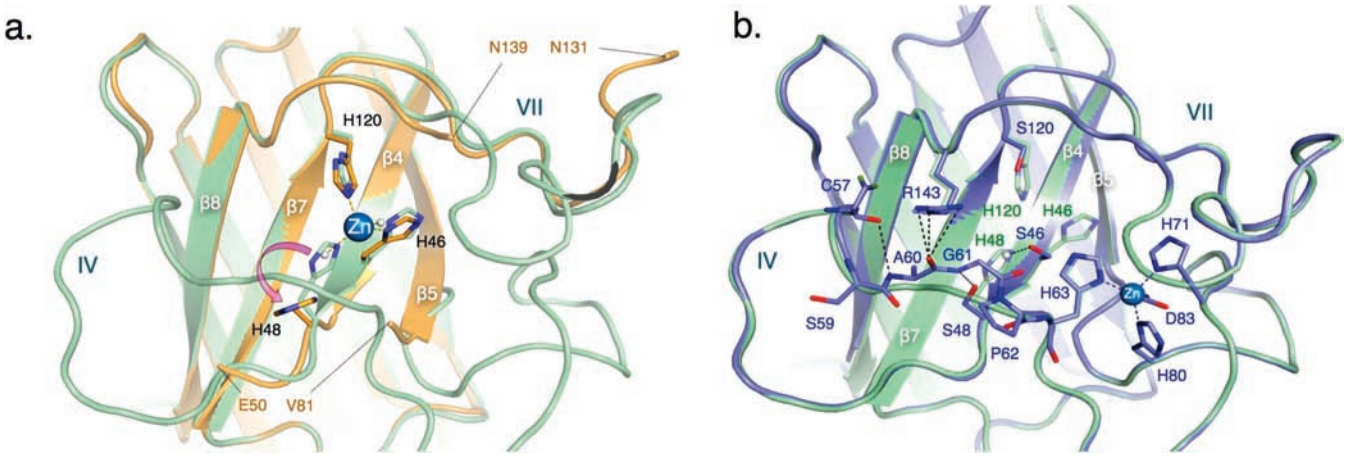

Figure 2. Structures of the SOD1 monomer with a single Zn^{2+} ion in the Cu site and Zn site. Moving a single Zn^{2+} ion between the Cu and Zn site has negligible effects on the SOD1 barrel but leads to local adjustments of the active-site loops. (a) Close-up of the holoSOD1^{CuX} structure (orange) showing that the coordination of Zn^{2+} to the Cu site in the absence of a metalated Zn site leads to misligation of H48.[3] The altered orientation of H48 is sterically incompatible with the native conformation of loop IV (50−81), which becomes disordered together with loop VII (131−139) in the crystal lattice. Superimposed is the ribbon representation of holoSOD1^{CuZn} (green) without the active-site metal ions; cf. Figure 1b. (b) Close-up of holoSOD1^{XZn} (blue) showing that coordination of Zn^{2+} to the native Zn site yields loop structures overall similar to those of holoSOD1^{CuZn} (green). A local difference is that residues 60−62 are rotated toward the Cu site due to the loss of steric repulsion caused by the H48S substitution. The hydrogen bonds that stabilize this local change of loop IV, as well as the water molecule interacting with the new orientation of S46, are indicated as dotted lines and a small white sphere, respectively.

on the Zn binding process in the wild-type protein, where both metal binding sites act in concert. When the denatured SOD1 monomer encounters a Zn^{2+} ion, this first catalyzes folding of the SOD1 barrel by coordinating transiently to the Cu site, then transfers to the Zn site, which is the thermodynamically most stable position. From an ALS perspective, the ability of Zn^{2+} to jump relatively swiftly between the Cu and Zn sites substantially increases the number of putative pathways to degradation and toxic function of SOD1 *in vivo*.

Results and Discussion

X-ray Structures of the holoSOD1 Monomer and the Variant without Cu Site. To target specifically how Zn^{2+} coordination affects the properties of the SOD1 monomer, we have based our measurements on the well-characterized pseudo-wild-type monomer with intact Cu and Zn ligands F50E/G51E/C6A/C111A (SOD1^{CuZn}).[12] Besides eliminating contributions from the dimer interface in the unfolding reaction, this mutant reduces the risk of erroneous disulfide cross-linking of denatured material under aerobic conditions.[12] The analysis includes three crystal structures, two of which are presented here for the first time. First, to obtain a structural reference for the holoSOD1 monomer, we have solved the crystal structure of the fully metalated pseudo-wild-type monomer with intact Cu and Zn ligands (holoSOD1^{CuZn}) at 1.45 Å resolution (Figure 1 and Table 1). The X-ray data show that the Cu and Zn ions are both well-ordered. Anomalous scattering data at four wavelengths establish

(12) Lindberg, M. J.; Normark, J.; Holmgren, A.; Oliveberg, M. *Proc. Natl. Acad. Sci. U.S.A.* **2004**, *101* (45), 15893–15898.

Table 1. Crystallographic Data Collection and Refinement Statistics (Values in Parentheses Correspond to the Highest Resolution Shell)

	holoSOD1^{CuZn}	holoSOD1^{XZn}
data collection statistics:		
space group	$P2_12_12_1$	$P2_12_12_1$
unit cell parameters (Å)	$a = 35.2$, $b = 49.5$, $c = 80.4$	$a = 34.8$, $b = 49.2$, $c = 80.5$
V_m (Å^3 Da^{-1})/solvent content (%)	2.22/44.6	2.21/44.3
resolution range (Å)	40.0−1.45 (1.49−1.45)	40.0−1.55 (1.59−1.55)
no. of measured reflections	189264 (11001)	171373 (8581)
no. of unique reflections	25245 (1851)	20574 (1478)
completeness (%)	98.6 (99.2)	99.4 (98.6)
R_{merge} (%)[a]	6.9 (66.4)	8.5 (61.9)
$I/\sigma(I)$	14.0 (2.8)	17.6 (3.3)
multiplicity	7.5 (6.0)	8.3 (5.8)
refinement and model statistics:		
resolution range (Å)	40.0−1.45 (1.49−1.45)	40.0−1.55 (1.59−1.55)
R_{model} (%)[b]	16.6 (26.7)	15.5 (26.8)
R_{free} (%)[c]	19.9 (27.9)	18.3 (28.8)
no. of residues	153	153
no. of water molecules	153	145
no. of ions/ligands	5	8
mean *B*-factor (Å^2) [protein (water)]	19.7 (39.7)	15.4 (36.0)
rms deviations from ideal geometry		
bond lengths (Å)	0.009	0.010
bond angles (°)	1.201	1.258
Ramachandran plot quality[d]:		
most favored (%)	89.3	88.5
additional allowed (%)	10.7	11.5

[a] $R_{merge} = \Sigma_{hkl}\Sigma_i|I(hkl)_i - \langle I(hkl)\rangle|/\Sigma_{hkl}\Sigma_i\langle I(hkl)_i\rangle$. [b] $R_{model} = \Sigma_{hkl}||F_o(hkl)| - |F_c|(hkl)|/\Sigma_{hkl}||F_o|(hkl)|$, where F_o and F_c are the observed and calculated structure factors. [c] R_{free} was calculated using 5.0% of the total reflections. [d] Calculated using PROCHECK.

the correct identity of the metal ions. In essence, the present holoSOD1^{CuZn} structure is identical to the atomic resolution structure of monomeric SOD1 (F50E/G51E/C6A/C111A/E133Q) crystallized in the presence of 200−400 mM Cd^{2+} (PDB entry 1MFM).[13] One difference is, however, that the Cu site ion in 1MFM is delocalized over two positions with approximately equal occupancies, separated by 1.6 Å, one of which contains Cd and the other Cu. This was interpreted as representing two binding sites, for Cu^{2+} and Cu^+, respectively.[13] In contrast, holoSOD1^{CuZn} shows only one Cu site density peak, located very close to the Cd^{2+} position in 1MFM (Figure 1) and thus represents a Cu^{2+} ion. However, the electron density has significant anisotropy (Supporting Information). The coordination sphere of Cu^{2+} has distorted square pyramidal geometry involving H46, H48, H63, H120, and one water molecule, the latter at a distance of 2.4 Å. This differs from the coordination in 1MFM, which contains two water molecules, at distances of 2.4 and 2.6 Å, respectively. However, it is much more similar to the geometry observed in the wild-type dimer[14] (1HL5), except that the water molecule is more tightly coordinated, at a distance of 2.4 Å rather than 2.7 Å. Likewise, the distorted tetrahedral geometry of the Zn^{2+} site in holoSOD1^{CuZn} is identical to that of the wild-type dimer.[15] On this basis, we conclude that holoSOD1^{CuZn} represents well the structure of the fully metalated wild-type protein.

Second, we have solved the crystal structure of the monomeric SOD1 variant in which the Cu site ligands H46, H48, and H120 have been mutated to S (holoSOD1^{XZn}). This construct is designed to reveal how the protein binds Zn^{2+} without interference from the native Cu ligands. The structure of holoSOD1^{XZn} was determined to 1.55 Å resolution (Table 1) and is overall isomorphous to that of holoSOD1^{CuZn} (Figure 2). The rms deviation in 139 Cα positions between the two structures is only 0.10 Å. The equivalent deviation between 1MFM and holoSOD1^{CuZn} is 0.18 Å. The structure of holoSOD1^{XZn} shows a single Zn^{2+} density coordinated in wild-type geometry by the native Zn^{2+} ligands H63, H71, H80, and D83, and the local perturbations at the Cu site as a result of the mutations are also minimal. The side chains of S48 and S120 imitate exactly the conformation of the H residues they replace, as far as the γ-atoms. Only the side chain of S46 is slightly rotated to make a H-bond to one of five water molecules that fill the space released by the mutations and the Cu loss (Figure 2).

As a consequence of engineering the wild-type species into monomeric form, part of loop IV (residues 53−61) loosens and becomes disordered.[1,4] In the holoSOD1^{XZn} structure, we can model an alternate conformation of residues 52−56 of loop IV in which they are oriented toward the β-barrel domain. This orientation of loop IV deviates between 3.4 and 5.2 Å in Cα positions from the conformation in holoSOD1^{CuZn} and could be the result of subtle changes in the crystal packing (Supporting Information). The most striking result of the Cu site truncation, however, is that the segment of loop IV that normally contacts H48 (residues 60−62) has rotated and collapsed inward (Figure 2).

Apparently, the removal of steric repulsion between His48-$N^{\delta1}$ and the amide nitrogen of Gly61 allows loop IV to twist to establish main-chain hydrogen bonds with the replacing S48 side chain and R143 (Figure 2). The overall structure of holoSOD1^{XZn}, including the active site loops, is essentially identical to the holo-wild-type protein. This is in stark contrast to previous observations that proteins with truncated Zn site (holoSOD1^{CuX}) suffer from extreme conformational disorder in the loop region[7,8] (Figure 2). In the absence of a natively coordinated Zn^{2+} ion, loops IV and VII unfold locally due to Zn^{2+} misligation at the Cu site and increase the protein's susceptibility to intermolecular association.[3] Consistent with previous results from solution NMR of the SOD1 monomer,[16] these observations demonstrate that metalation of the SOD1 Zn site is the principal factor for stabilizing the active-site loops in their correct native geometry.

Truncation of the Cu Ligands: Impact on Folding and Stability of the apoSOD1 Monomer. As is typical for globular proteins,[17] apoSOD1^{CuZn} and apoSOD1^{XZn} display a two-state folding process with a classically V-shaped chevron plot[12,18] (Figure 3). Characteristic for these plots is that the logarithmized refolding and unfolding rate constants (log k_f and log k_u) display linear dependences on [urea] (eqs 8 and 9), indicating that the unfolded ensemble (U), the folding transition state (‡), and the folded state (F) are structurally robust and do not change upon addition of denaturant. A particular advantage of such linear chevron plots is that the unfolding rate constant (k_u) can be

(13) Ferraroni, M.; Rypniewski, W.; Wilson, K. S.; Viezzoli, M. S.; Banci, L.; Bertini, I.; Mangani, S. *J. Mol. Biol.* **1999**, *288* (3), 413–426.
(14) Strange, R. W.; Antonyuk, S.; Hough, M. A.; Doucette, P. A.; Rodriguez, J. A.; Hart, P. J.; Hayward, L. J.; Valentine, J. S.; Hasnain, S. S. *J. Mol. Biol.* **2003**, *328* (4), 877–891.
(15) Hart, P. J.; Liu, H.; Pellegrini, M.; Nersissian, A. M.; Gralla, E. B.; Valentine, J. S.; Eisenberg, D. *Protein Sci.* **1998**, *7* (3), 545–555.
(16) Banci, L.; Bertini, I.; Cantini, F.; D'Onofrio, M.; Viezzoli, M. S. *Protein Sci.* **2002**, *11* (10), 2479–2492.
(17) Oliveberg, M.; Wolynes, P. G. *Q. Rev. Biophys.* **2005**, *38* (3), 245–288.
(18) Svensson, A. K.; Bilsel, O.; Kondrashkina, E.; Zitzewitz, J. A.; Matthews, C. R. *J. Mol. Biol.* **2006**, *364* (5), 1084–1102.

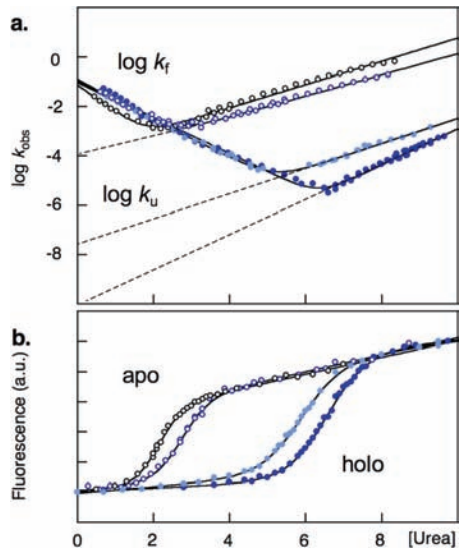

Figure 3. Effects on folding and stability of Cu ligand substitution and coordination of Zn^{2+} to the native Zn ligands. apoSOD1^{CuZn} (open black), apoSOD1^{XZn} (open blue), holoSOD1^{XZn} "as-purified" (pale blue), and holoSOD1^{XZn} in 500 μM $ZnCl_2$ (blue). (a) Chevron plots of log k_{obs}= log(k_f + k_u) vs [urea] (eq 11). The coordination of Zn^{2+} to SOD1^{XZn} has no detectable effect on the refolding rate constant (k_f) but decreases the unfolding rate constant (k_u). This suggests that Zn^{2+} binds selectively to the folded state, consistent with the Zn^{2+} concentration dependence of log k_u. The dotted lines show the extrapolation of log k_u to [urea] = 0 M. (b) Corresponding equilibrium unfolding data. The kinetic and thermodynamic parameters obtained from the data in panels a and b are listed in Table 2.

accurately extrapolated to [urea] = 0 M and used to estimate protein stability and native state lifetimes ($1/k_u$) in pure physiological buffer (eq 11). The results for apoSOD1^{XZn} show that mutation of the Cu ligands H46, H48, and H120 to S has no appreciable effect on the V-shaped nature of the chevron plot. This indicates that the folding reaction of apoSOD1^{XZn} remains wild-type-like. Even so, the mutations cause a marked increase in stability in apoSOD1^{XZn} relative to the pseudo-wild-type monomer. The transition midpoint as derived from kinetic data increases from 1.9 to 2.6 M urea, corresponding to a stability gain of $\Delta\Delta G_{U/F} = 0.6$ kcal/mol (Table 2). Interestingly, a very similar increase in stability is found when cutting back the neighboring Zn^{2+} ligands in apoSOD1^{CuX} through the quadruple mutation H63S/H71S/H80S/D83S.[3] Although the molecular basis for this stability increase is not yet clear, this recurrent phenomenon suggests that the acquisition of metal binding ligands in SOD1 has come at a cost: optimization of function and structure occur sometimes occur in conflict.[3,19−21]

Removal of the Cu site affects both the refolding and unfolding limbs of the chevron plot: refolding becomes faster and unfolding slows down (Figure 3). This response is characteristic for mutations of side chains that experience a partly native-like environment at the top of the folding barrier (‡).[22] Such an early assembly of the Cu site in the SOD1 folding process is fully consistent with the finding that β4 and β7, which form the anchoring points for the Cu ligands, are part of the folding nucleus.[23] The response also goes hand-in-hand with the observation that both Cu^{2+} and Zn^{2+} ions are able to bind to the SOD1 Cu site in the folding transition state, catalyzing the folding reaction through a nearly hundred-fold increase of k_f[3] (Figure 4).

Zn^{2+} Binding Stabilizes Selectively the Folded SOD1 Monomer and Increases Its Lifetime by Hundreds of Years. Coordination of Zn^{2+} to SOD1^{XZn} yields a pronounced effect on the unfolding kinetics (Figure 3): k_u decreases from 6.9×10^{-5} to 2.6×10^{-8} s^{-1}, corresponding to an increase in protein stability of $\Delta\Delta G_{U/F} \approx 4.5$ kcal/mol at stoichiometric amounts of Zn^{2+} ions (Table 2). Notably, the Zn^{2+} binding shows no appreciable effect on the refolding rate constant (k_f), indicating that the stability gain is restricted to the native state (Figure 3). Thus, in clear contrast to SOD1^{CuX}, where metalation of the Cu ligands yields a pronounced effect on k_f (Figure 4 and Table 2), the Zn site of SOD1^{XZn} seems not to interact with Zn^{2+} in the folding transition state. Even so, it cannot be excluded that the Zn^{2+} ion interacts with loop IV already in the denatured state[4] and is then carried along as a "satellite" outside the folding nucleus that docks to the SOD1 framework only at the very end of the folding process. In such a case, the effect on k_f would be small because the free-energy perturbations of U and ‡ are very similar. Although FRET analysis has previously demonstrated that Zn^{2+} ions are indeed able to interact with the native ligands in disordered loop IV peptides,[4] we favor here the interpretation that Zn^{2+} is lost from the SOD1^{XZn} structure prior to the global unfolding event

$$[U] \underset{k_u^{apo}}{\overset{k_f^{apo}}{\rightleftharpoons}} [F^{apo}] + [Zn^{2+}] \underset{k_{off}^{Zn}}{\overset{k_{on}^{Zn}}{\rightleftharpoons}} [F^{holo}] \quad \text{(Scheme1)}$$

where k_{on}^{Zn} and k_{off}^{Zn} are the rate constants for Zn^{2+} binding and Zn^{2+} dissociation, respectively. Consistent with this assumption, the unfolding time course is also seen to deviate from exponentiality at stoichiometric concentrations of Zn^{2+}, as expected from a second-order component in the ground state (Supporting Information). This second-order component disappears at higher concentrations of Zn^{2+} as unfolding becomes pseudo-first-order; that is, the concentration of free Zn^{2+} remains approximately constant during the unfolding process. It is nevertheless clear that Zn^{2+} binding has a radical influence on the lifetime of the folded state as extrapolated to 0 M urea. The value of $1/k_u$ increases from 4 h for apoSOD1^{XZn} to 1.2 years for holoSOD1^{XZn} (Figure 3, Table 2). This lifetime increases further to more than 600 years upon increasing the Zn^{2+} concentration to 500 μM, as expected from mass action and selective binding to the folded state (Figure 3, Table 2). From a physiological perspective, however, such long lifetimes are unrealistic. Even if holoSOD1 stands out as a most durable protein by maintaining full enzymatic activity for >120 days in erythrocytes (S. Marklund, personal communication), the in vitro lifetimes for other proteins are usually much shorter[24] (Figure 5).

Regulatory proteins like transcription factors have short lifetimes (s) to allow rapid turnover, whereas a "typical" globular protein shows a lifetime of hours to days,[25] in good accord with

(19) Sutto, L.; Latzer, J.; Hegler, J. A.; Ferreiro, D. U.; Wolynes, P. G. *Proc. Natl. Acad. Sci. U.S.A.* **2007**, *104* (50), 19825–19830.
(20) Gosavi, S.; Whitford, P. C.; Jennings, P. A.; Onuchic, J. N. *Proc. Natl. Acad. Sci. U.S.A.* **2008**, *105* (30), 10384–10389.
(21) Friel, C. T.; Smith, D. A.; Vendruscolo, M.; Gsponer, J.; Radford, S. E. *Nat. Struct. Mol. Biol.* **2009**, *16* (3), 318–324.
(22) Fersht, A. R. Structure and Mechanism in Protein Science: A Guide to Enzyme Catalysis and Protein Folding; WH Freeman: New York, 1999.
(23) Nordlund, A.; Oliveberg, M. *Proc. Natl. Acad. Sci. U.S.A.* **2006**, *103* (27), 10218–10223.
(24) Jackson, S. E. *Fold Des.* **1998**, *3* (4), R81–R91.
(25) Maxwell, K. L.; et al. *Protein Sci.* **2005**, *14* (3), 602–616.

Table 2. Kinetic and Thermodynamic Data (Rate Constants Are in Units of s^{-1})

	apoSOD1^{CuZn}	apoSOD1^{XZn}	holoSOD1^{XZn} as-purified	holoSOD1^{XZn} 500 μM $ZnCl_2$	holoSOD1^{CuX} 500 μM $ZnCl_2$
$\log k_f^{H_2O}$ [a]	-1.16 ± 0.1	-0.9 ± 0.06	-1.04 ± 0.03	-1.04 ± 0.05	0.76 ± 0.02
$\log k_u^{H_2O}$ [a]	-4.01 ± 0.05	-4.16 ± 0.05	-7.59 ± 0.12	-10.35 ± 0.21	-4.7 ± 0.12
m_f [a]	-1.03 ± 0.09	-0.83 ± 0.04	-0.75 ± 0.01	-0.72 ± 0.02	-0.81 ± 0.01
m_u [a]	0.49 ± 0.01	0.43 ± 0.01	0.51 ± 0.02	0.75 ± 0.03	0.22 ± 0.01
$\log k_{off}^{H_2O}$ in ZINPYR-1 [b]			-4.84 ± 0.14		
$\log k_{off}^{H_2O}$ in EDTA [b]			-4.64 ± 0.06		-2.33 ± 0.04 [e]
$\log k_{off}^{H_2O}$ in EDTA [c]			-5.23 ± 0.02		
m_{off} in ZINPYR-1 [b]			0.23 ± 0.02		
m_{off} in EDTA [b]			0.21 ± 0.01		0.07 ± 0.01 [e]
$m_{D/N}^{kin}$ [a]	1.51 ± 0.09	1.26 ± 0.04	1.26 ± 0.02	1.46 ± 0.03	1.03 ± 0.03
$m_{D/N}^{eq}$ [d]	1.32 ± 0.09	1.21 ± 0.07	0.89 ± 0.03	0.98 ± 0.03	0.84 ± 0.05 [f]
MP^{kin} (M) [a]	1.88 ± 0.07	2.59 ± 0.05	5.19 ± 0.04	6.37 ± 0.06	5.33 ± 0.06
MP^{eq} (M) [d]	2.12 ± 0.05	2.73 ± 0.04	5.79 ± 0.02	6.45 ± 0.02	5.85 ± 0.05 [f]
ΔG^{kin} (kcal mol^{-1}) [a]	3.87 ± 0.15	4.44 ± 0.1	8.93 ± 0.17	12.69 ± 0.29	7.47 ± 0.14
ΔG^{eq} (kcal mol^{-1}) [d]	3.81 ± 0.2	4.49 ± 0.18	7.06 ± 0.1	8.58 ± 0.1	6.7 ± 0.18 [f]

[a] Derived from kinetic data in Figures 3a, 4a, and eq 11. [b] Derived from log k_u measured in the presence of chelator (Figure 6a) by linear extrapolation to 0 M urea. [c] Derived from double-jump experiments in Figure 6b. [d] Derived from equilibrium data in Figure 3b and eq 10. [e] Data from holoSOD1^{CuX} as purified in Figure 6a. [f] Extracted from ref 3.

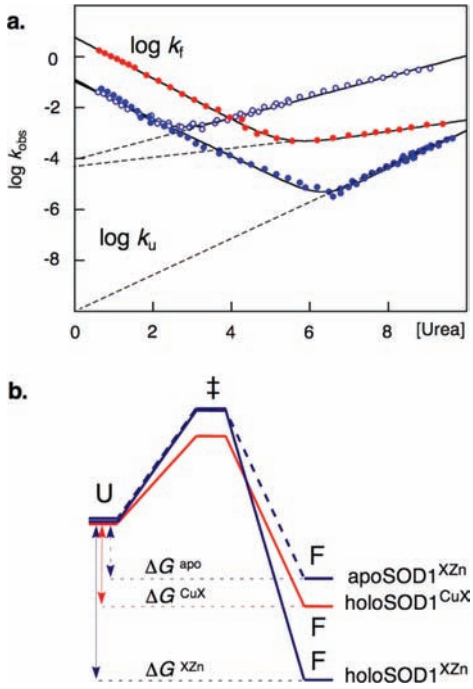

Figure 4. Zn^{2+} binding to the SOD1 Cu ligands occurs early in folding and stabilizes the folding transition state, whereas Zn^{2+} binding to the native Zn ligands occurs late in folding and stabilizes selectively the folded state. (a) Chevron plots of the SOD1 monomer with Zn^{2+} in the Zn site (holoSOD1^{XZn}, closed blue) and Zn^{2+} in the Cu site (holoSOD1^{CuX}, closed red), respectively. The reference for the apo monomer is apoSOD1^{XZn} (open blue). Metalation of the Cu ligands increases the folding rate constant (log k_f), whereas metalation of the Zn ligands has no effect on log k_f but decreases selectively the unfolding rate constant (log k_u). (b) Folding free-energy profiles showing the corresponding stabilities of the unfolded state (U), the folding transition state (‡), and the folded state (F). Zn^{2+} binding to the SOD1 Cu ligands catalyzes folding by lowering the free energy of ‡. In contrast, Zn^{2+} binding to the native Zn ligands has no effect on the barrier for folding.

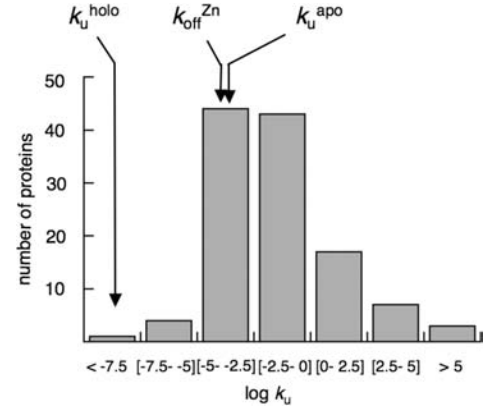

Figure 5. Histogram of unfolding rate constants of globular proteins obtained from data in ref 24 and http://kineticdb.protres.ru/db/index.pl. By comparison, the lifetime of holoSOD1^{XZn} sticks out as exceptionally long ($1/k_u^{holo} \approx 15$ months for as-purified material and 726 years in the presence of 500 μM Zn^{2+}), whereas the lifetime of apoSOD1^{XZn} is within the normal range ($1/k_u^{apo} \approx 4$ h). However, unfolding of holoSOD1^{XZn} becomes much faster ($1/k_{off}^{Zn} \approx 22$ h, cf. Figure 6) if dissociated Zn^{2+} is prevented from rebinding to the folded state; i.e., holoSOD1 is made into apoSOD1. Thus, Zn^{2+} depletion stands out as a possible pathway to rapid unfolding and degradation *in vivo*.

that of apoSOD1. A classical example of proteins with lifetimes in excess of several years are the extracellular bacterial serine proteases.[26] The long functional lifetimes are here maintained by a selective elevation of the folding barrier that is decoupled from the protein stability.[27] The long lifetime of holoSOD1^{XZn}, on the other hand, is directly linked to an increase in protein stability. A more suitable comparison is thus the exceptionally long lifetimes (>1000 years) estimated for the metal-containing ferrodoxins in thermophilic bacteria.[28] For these proteins, the slow unfolding kinetics at room temperature are suggested to stem from their high thermal stability;[28] at the extreme temperatures where the bacteria live, the lifetimes are likely to be considerably shorter. The question then arises: why does the holoSOD1 molecule need to be so stable against unfolding under physiological conditions, and what factors control its cellular turnover?

Zn Off Rate Is Much Faster than the Holo Unfolding Rate Constant: A Shortcut to Rapid Degradation in Vivo? To examine more closely the role of Zn^{2+} in SOD1^{XZn} unfolding, we measured the effect of chelators on the unfolding rate constant, k_u. The idea of this experiment was to estimate the

(26) Jaswal, S. S.; Sohl, J. L.; Davis, J. H.; Agard, D. A. *Nature* **2002**, *415* (6869), 343–346.

(27) Cunningham, E. L.; Jaswal, S. S.; Sohl, J. L.; Agard, D. A. *Proc. Natl. Acad. Sci. U.S.A.* **1999**, *96* (20), 11008–11014.

(28) Wittung-Stafshede, P. *Biochim. Biophys. Acta* **2004**, *1700* (1), 1–4.

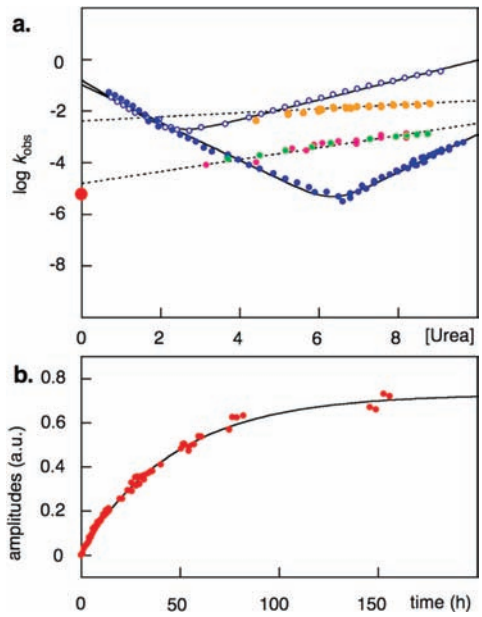

Figure 6. Unfolding of SOD1 in the presence of chelators shows that the rate constants of Zn^{2+} dissociation (log k_{off}^{Zn}) from the Zn and Cu sites are faster than global unfolding of the holo proteins (log k_u). (a) Unfolding of holoSOD1^{XZn} in the presence of EDTA (green) and ZINPYR-1 (magenta) is faster than unfolding of protein in urea with zinc (blue). The increased unfolding rate constants are the same and yield a direct measure of k_{off}^{Zn} according to *Scheme 1*; if dissociated Zn^{2+} is prevented from rebinding to the Zn site, global unfolding becomes rate limited by k_{off}^{Zn}. The value of k_{off}^{Zn} at 0 M urea (red) is derived from the double-jump experiments in panel b. Dissociation of Zn^{2+} from the SOD1 Cu site is even faster as measured by unfolding of holoSOD1^{CuX} in the presence of EDTA (orange). Notably, log k_u of holoSOD1^{CuX} in the presence of EDTA converges with the unfolding limb of the apoSOD1 monomer at ~6 M urea. Below this urea concentration, the rate-limiting step shifts from k_{off}^{Zn} to unfolding of the apo monomer. (b) Time course for dissociation of Zn^{2+} from holoSOD1^{XZn} at 0 M urea, measured by the production of apo protein in the presence of excess amounts of EDTA. The extent of apo protein produced at each time point was estimated from the apo unfolding amplitude at 8.25 M urea.

rate constant of Zn^{2+} dissociation from the folded state (k_{off}^{Zn}).[6,29] We used two types of chelators: ZINPYR-1, which shows a fluorescence increase upon Zn^{2+} binding, and EDTA, which is spectroscopically silent in the kinetic experiment. Both chelators were added in excess to achieve final concentrations of 2.6 μM ZINPYR-1 per 1.3 μM as-purified SOD1^{XZn} monomer and 500 μM EDTA per 5 μM as-purified SOD1^{XZn} monomer. The results show that the effects of ZINPYR-1 and EDTA are the same: the unfolding reaction becomes faster and the m_u value decreases (Figure 6 and Table 2).

Upon extrapolation of data to 0 M urea, we obtain an apparent unfolding rate constant of 1.9×10^{-5} s^{-1}, which is in good accord with previous findings for the wild-type dimer.[6] As a control of this extrapolation, we followed also, by double mixing, how EDTA scavenges Zn^{2+} from folded SOD1^{XZn} at 0 M urea. This direct measurement yields a rate constant $k_{off}^{Zn} = 0.6 \times 10^{-5}$ s^{-1}, which is in good agreement with the extrapolated value. On this basis, we conclude that the chelators measure directly the values of k_{off}^{Zn}. The affinity for Zn^{2+} (K_{diss}^{Zn}) to the folded SOD1 monomer (F) is then given by

$$K_{diss}^{Zn} = k_{off}^{Zn}/k_{on}^{Zn} = [F^{apo}][Zn^{2+}]/[F^{holo}] \quad (1)$$

where k_{on}^{Zn} is the second-order rate constant for Zn^{2+} association. As K_{diss}^{Zn} is likely to be less than 10^{-9} in physiological buffer,[6,30,31] the value of k_{on}^{Zn} must be orders of magnitudes higher than k_{off}^{Zn}. Thus, under the experimental conditions, k_{on}^{Zn} appears faster than global unfolding of the apo protein and the binding and release of Zn^{2+} can be treated as a rapid pre-equilibrium in the global unfolding reaction, as depicted in *Scheme 1*. Moreover, the positive urea dependence of log k_{off}^{Zn} (m_{off}^{Zn}) indicates that the Zn^{2+} dissociation is accompanied by local unfolding. This is in good accord with the quite buried position of the Zn site in the SOD1 structure: release of Zn^{2+} requires opening of the active-site loops. It is also possible that the increased value of k_{off}^{Zn} at high [urea] is coupled to reduced Zn^{2+} affinity. Assuming that the reduction is manifested entirely in k_{off}^{Zn}, K_{diss}^{Zn} increases 10-fold between 0 and 8 M urea. For comparison, dissociation of Zn^{2+} from the SOD1 Cu site in SOD1^{CuX} is observed to be considerably faster and has a lower m_{off}^{Zn} (Figure 6 and Table 2), fully consistent with its more solvent-accessible position in the holoSOD1^{CuX} structure (Figure 2). When it comes to the physiological lifetime of folded SOD1, however, the relatively fast, spontaneous dissociation of Zn^{2+} provides an alternative, more rapid pathway to degradation. Under conditions where the Zn^{2+} ion is prevented from instant rebinding, for example, if it becomes chelated by a neighboring protein in vivo, the Zn^{2+} free protein will readily unfold on time scales typical for globular proteins: dissociation of the Zn^{2+}-depleted SOD1 dimers takes place with rate constants in excess of 10^{-5},[12,32] and the subsequent unfolding of the monomers occurs on similar time scales (Table 2). Hence, the removal of the native Zn^{2+} ion not only controls loop dynamics[3,33] and interface strength[34] but also reduces the lifetime of the folded protein from years to less than 25 h (Figures 5 and 6). *In vivo*, this pathway to degradation is expected to be promoted even further by protonation of the histidine ligands upon transfer into the acidic macroautophagosome/lyzosome complex.[35]

Changes of Zn^{2+} Affinity and Zn^{2+} Buffering by Urea Add New Components to the Chevron *m* Values. From the chevron plots in Figure 3, it can be seen that the slope of the unfolding limb (m_u) of SOD1^{XZn} undergoes a significant increase upon coordination of Zn^{2+}. The effect is particularly pronounced at 500 μM Zn^{2+}, where m_u becomes 0.32 units higher than for the apo protein (Table 2). A common explanation for this phenomenon is that the change in solvent-accessible surface area between the transition state (‡) and the folded ground state (F) has increased. This could happen either by ‡ shifts[17,36] according to Hammond postulate behavior[37] or by structural consolidation of F.[38,39] In the latter case, the SOD1 molecule would become more consolidated as Zn^{2+} binding freezes the dynamic motions

(29) Mulligan, V. K.; Kerman, A.; Ho, S.; Chakrabartty, A. *J. Mol. Biol.* **2008**, *383* (2), 424–436.
(30) Kayatekin, C.; Zitzewitz, J. A.; Matthews, C. R. *J. Mol. Biol.* **2010**, *398* (2), 320–331.
(31) Potter, S. Z.; Zhu, H.; Shaw, B. F.; Rodriguez, J. A.; Doucette, P. A.; Sohn, S. H.; Durazo, A.; Faull, K. F.; Gralla, E. B.; Nersissian, A. M.; Valentine, J. S. *J. Am. Chem. Soc.* **2007**, *129* (15), 4575–4583.
(32) Khare, S. D.; Caplow, M.; Dokholyan, N. V. *Proc. Natl. Acad. Sci. U.S.A.* **2004**, *101* (42), 15094–15099.
(33) Teilum, K.; Smith, M. H.; Schulz, E.; Christensen, L. C.; Solomentsev, G.; Oliveberg, M.; Akke, M. *Proc. Natl. Acad. Sci. U.S.A.* **2009**, *106* (43), 18273–18278.
(34) Hornberg, A.; Logan, D. T.; Marklund, S. L.; Oliveberg, M. *J. Mol. Biol.* **2007**, *365* (2), 333–342.
(35) Nixon, R. A.; Cataldo, A. M. *Trends Neurosci.* **1995**, *18* (11), 489–496.
(36) Oliveberg, M. *Acc. Chem. Res.* **1998**, *31* (11), 765–772.
(37) Hammond, G. S. *J. Am. Chem. Soc.* **1955**, *77*, 334–338.
(38) Otzen, D. E.; Oliveberg, M. *J. Mol. Biol.* **2002**, *317* (4), 639–653.
(39) Oliveberg, M. *Curr. Opin. Struct. Biol.* **2001**, *11* (1), 94–100.

of the active-site loops. Although such ground-state alterations are certainly consistent with NMR data,[33,40] we favor in this study a more general interpretation based on the urea dependence of the Zn^{2+} affinity (K_{diss}^{Zn}) indicated by the positive value of $m_{off}^{Zn} = \partial \log k_{off}^{Zn}/\partial[\text{urea}]$ (eq 1, Figure 6). Our motivation is that (i) it serves to illustrate how the *m* values of metalloproteins can include contributions beyond changes in solvent-accessible surface area, and (ii) depending on the source of the K_{diss}^{Zn} change, the interpretation can still, but does not need to, be compatible with structural alterations of the ground state. The rationalization is as follows. From *Scheme 1* and $k_{on}^{Zn} > k_u^{apo}$, the observed unfolding rate constant can be written

$$k_u^{obs} = k_u^{apo} f^{apo} \tag{2}$$

where $f^{apo} = [F^{apo}]/([F^{apo}] + [F^{holo}])$ is the fraction of folded apoSOD1^{XZn} molecules in the pre-equilibrium. Accordingly

$$\begin{aligned} &\log k_u^{obs} = \log k_u^{apo} + \log f^{apo} \Rightarrow \\ &\log k_u^{obs,H_2O} + m_u^{obs}[\text{urea}] = \\ &\log k_u^{apo,H_2O} + m_u^{apo}[\text{urea}] + \log f^{apo}, \log f^{apo,H_2O} + m_{fraction}^{apo}[\text{urea}] \end{aligned} \tag{3}$$

which yields two components to the observed m_u value

$$m_u^{obs} = m_u^{apo} + m_{fraction}^{apo} \tag{4}$$

where $m_{fraction}^{apo} = \partial \log f^{apo}/\partial[\text{urea}]$. It then follows from eq 1 that

$$\begin{aligned} &k_{off}^{Zn} = k_{on}^{Zn} K_{diss}^{Zn} = k_{on}^{Zn}[F^{apo}][Zn^{2+}]/[F^{holo}] \Rightarrow \\ &\log k_{off}^{Zn} = \log k_{on}^{Zn} + \log[F^{apo}]/[F^{holo}] + \log[Zn^{2+}] \Rightarrow \\ &\log k_{off}^{Zn} \approx \log k_{on}^{Zn} + \log f^{apo} + \log[Zn^{2+}] \text{ and } m_{off}^{Zn} \approx \partial \log f^{apo}/\partial[\text{urea}] \end{aligned} \tag{5}$$

assuming that $[F^{apo}] \ll [F^{holo}]$, and $\partial \log k_{on}^{Zn}/\partial[\text{urea}]$ and $\partial \log [Zn^{2+}]/\partial[\text{urea}]$ are relatively small. Taken together, eqs 4 and 5 yield

$$m_u^{obs} = m_u^{apo} + m_{off}^{Zn} \tag{6}$$

Comparison with the experimental data shows that the value $m_{off}^{Zn} = 0.21-0.23$ matches fairly well the m_u change upon Zn^{2+} binding, that is, $m_u^{obs} - m_u^{apo} = 0.32 \pm 0.03$ at $[Zn^{2+}] = 500$ μM where unfolding is pseudo-first-order (Table 2). However, there is another contribution to m_u^{obs} in mixed solutions of urea and Zn^{2+}, which could make the agreement even better. Urea displays a significant Zn^{2+} binding capacity[41,42] that will decrease the effective concentration of Zn^{2+} ions at high [urea], that is, $\partial \log[Zn^{effective}]/\partial[\text{urea}] < 0$. Such a urea-promoted Zn^{2+} gradient expands eq 6 to

$$m_u^{obs} = m_u^{apo} + m_{off}^{Zn} + m_{[Zn]} \tag{7}$$

where $m_{[Zn]} = -\partial \log[Zn^{effective}]/\partial[\text{urea}]$ since f^{apo} increases linearly with decreasing $[Zn^{effective}]$ (eq 1). This contribution is expected to increase m_u^{obs} even further. Hence, it is not justified to invoke changes of solvent-accessible surface area as the sole source for the increased m_u of holoSOD1^{XZn}, even though such structural components are likely to be part of the effect. Although quantification of these different m_u components is presently difficult, their very existence should be kept in mind when interpreting chevron data from metalloproteins.

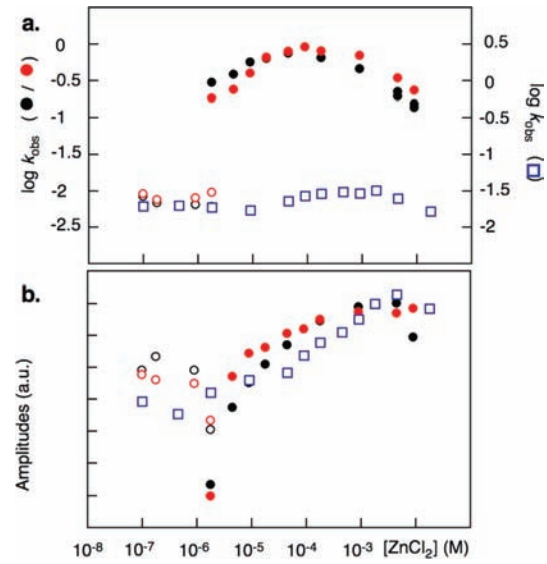

Figure 7. Wild-type monomer SOD1^{CuZn} folds by coordinating Zn^{2+} to the native Cu ligands, in precisely the same way as SOD1^{CuX}. (a) Dependence on $[Zn^{2+}]$ of the refolding rate constant (log k_f) at 1.06 M urea. The wild-type monomer SOD1^{CuZn} (black) shows a titration plot indistinguishable from that of SOD1^{CuX} (red): at low $[Zn^{2+}]$, the refolding rate constants match those of the apo protein (open circles), and above $[Zn^{2+}] \approx 2$ μM, they increase to the values of the protein with Zn^{2+} in the Cu site (closed circles). SOD1^{XZn}, which lacks the Cu site, shows the apo k_f at all concentrations of Zn^{2+} (open blue squares). (b) Corresponding refolding amplitudes show a titration midpoint at $[Zn^{2+}] \approx 2$ μM for both SOD1^{CuZn} and SOD1^{CuX}. At this midpoint, the refolding time course is biphasic.

Non-native Zn^{2+} Coordination Catalyzes Wild-Type Folding. From the chevron data in Figure 4, it is evident that the effect of Zn^{2+} on the SOD1 folding reaction depends very much on where it binds. Coordination of Zn^{2+} to the Cu ligands H46 and H120 (Figure 2) seems to take place already in the denatured state and stabilizes the folding transition state by bringing together β strands 4 and 7.[3,23] As a consequence, the refolding rate constant increases from log $k_f^{H_2O} = -1.16$ to log $k_f^{H_2O} = 0.76$ (Figure 4 and Table 2). In clear contrast, the native Zn^{2+} ligands H63, H71, H80, and D83 (Figure 2) seem unable to coordinate their ion before the protein is folded. However, once the active-site loops have been brought into a native-like topology, the binding of Zn^{2+} to the SOD1 Zn site becomes strong, with an off rate that is more than 200 times slower than for the lower affinity Cu site (Figure 6 and Table 2). The question is then whether the data from SOD1^{CuX} and SOD1^{XZn} can be combined to delineate how Zn^{2+} affects folding of wild-type SOD1, where the two competing Zn^{2+} binding sites act in concert. As a test, we measured how a gradual increase of the solvent Zn^{2+} concentration affects the refolding rate constant of SOD1^{CuZn}. The results show that the refolding rate constant of SOD1^{CuZn} undergoes a distinct increase around stochiometric amounts of Zn^{2+} (1−4 μM), indicating early coordination of Zn^{2+} ions (Figure 7). Notably, the observed $[Zn^{2+}]$ dependence of k_f is indistinguishable from that of SOD1^{CuX} (Figure 7), showing that the wild-type monomer also folds by coordinating Zn^{2+} to its Cu ligands at micromolar Zn^{2+} concentrations.

(40) Banci, L.; Bertini, I.; Boca, M.; Calderone, V.; Cantini, F.; Girotto, S.; Vieru, M. *Proc. Natl. Acad. Sci. U.S.A.* **2009**, *106* (17), 6980–6985.
(41) Ozutsumi, K.; Taguchi, Y.; Kawashima, T. *Talanta* **1995**, *42* (4), 535–541.
(42) Huh, Y. S.; Yang, K.; Hong, Y. K.; Jun, Y.-S.; Hong, W. H.; Kim, D. H. *Process Biochem.* **2007**, *42*, 649–654.

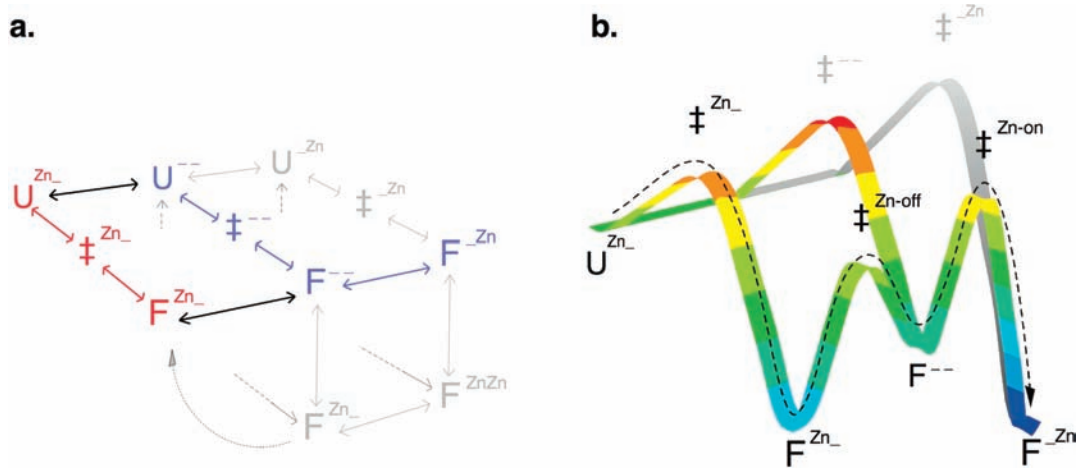

Figure 8. Simplistic free-energy landscape, illustrating the mechanism of folding-induced Zn^{2+}transfer. (a) Zn^{2+} binding to the Cu and Zn site of the SOD1 monomer is described by a cubic scheme with four unfolded (U) and folded (F) species, separated by folding transition states (‡). These species represent all the combinatorial variants of metalation for a protein with two metal binding sites: apo states with empty Cu and Zn sites (− −), states with Zn^{2+} in the Cu site and empty Zn site (Zn_), states with empty Cu site and Zn^{2+} in Zn site (_Zn), and fully metalated states with Zn^{2+} in both Cu and Zn site (Zn Zn). To emphasize the free energies controlling the binding of a single Zn^{2+} ion, we exclude the doubly metalated pathway $U^{Zn\ Zn} \leftrightarrow ‡^{Zn\ Zn} \leftrightarrow U^{Zn\ Zn}$. This allows us to convert the binding cube to a plane where the folding pathways for holoSOD1^{CuX} and holoSOD1^{XZn} are highlighted red and blue, respectively (cf. Figure 4). (b) Free-energy landscape of the planar binding scheme in panel a, illustrating how a single Zn^{2+} ion first catalyzes the folding reaction by binding transiently to the Cu ligands, and then transfers to its thermodynamically most stable position in the Zn site (dotted arrow). Free energies are calculated from the folding free-energy profiles in Figure 4 and the k_{off}^{Zn} values in Figure 6, assuming a prefactor of 10^6 s^{-1}.[17] The free energies of the unfolded states have been adjusted to a Zn^{2+} concentration where $[U^{Zn\_}]/[U^{--}] = 1$, and the undetectable pathway via U^{-Zn} and $‡^{-Zn}$ is tentatively shown in gray.

This promiscuous behavior of the Cu ligands in wild-type SOD1 reconciles some apparently conflicting data in the literature: refolding of wild-type SOD1 with a preloaded Zn site,[4] that is, one Zn^{2+} per monomer, yields a rate constant identical to that of holoSOD1^{CuX}.[3] Although the native Zn site ultimately has the highest affinity for the Zn^{2+} ion, binding to the SOD1 Cu site offers a kinetic advantage by speeding up the folding reaction. This finding goes hand in hand with the earlier observation that mutational introduction of histidine pairs that span contacts within the folding nucleus of ubiquitin and the GCN4 coiled coil domain generally increases the folding rate in the presence of divalent ions.[43,44] In the case of SOD1, however, non-native coordination of Zn^{2+} to the protein's natural Cu ligands acts as an inherent catalyst for folding.

Folding-Induced Zn^{2+} Transfer. The function of the Cu ligands in catalyzing folding of the SOD1 monomer leads inevitably to the second question: what happens to the Zn^{2+} ion after the protein has passed the folding transition state? The simple answer is that it transfers to the neighboring Zn site which, after all, is the thermodynamically most favorable position[10,31] (Figure 8). Exactly how this occurs is not yet clear, however. Under the experimental conditions, where the proteins are subject to a reservoir of free Zn^{2+} ions, it is likely that a second Zn^{2+} will bind as soon as the molecule is folded since Zn^{2+} binding to folded SOD1 seems generally faster than folding. This, in turn, will lead to transient mix of fully metalated and apo species that equilibrates to a uniform distribution of species with just one Zn^{2+} in the Zn site on longer time scales. Depending on the rate of intermolecular ion transfer in the folded SOD1 molecules, the second Zn^{2+} will here either refill the Cu site or enter directly into the Zn site, precluding the actual transfer reaction. At present, we cannot distinguish between these possibilities. Nevertheless, the propensity of the Zn^{2+} to end up transiently in the low-affinity Cu site adds an interesting twist to the situation in vivo where there is very little free Zn^{2+} available[45] and where further metalation is limited by the off rates from competing Zn^{2+} sites in other macromolecules. Under such conditions, the increased effective concentration of Zn^{2+} provided by a Zn^{2+}-loaded Cu site is likely to favor intermolecular ion transfer to the neighboring, native Zn site. Although the in vivo loading of Cu ions is known in many cases to involve the chaperone CCS, it is yet uncertain how Zn^{2+} enters the apo protein inside the cell.[46−48] On the basis of the current results, it can even be conceived that the relatively solvent-accessible Cu site acts as a natural shuttle for Zn^{2+} loading of the SOD1 molecule. In particular, if Zn^{2+} coordination of the native Zn^{2+} ligands involves structural rearrangements of the active-site loops as implicated by NMR,[49,50,3,33] m_u changes (Figures 3, 4, and 6) and crystallographic data (Figure 2).

Conclusions

In this study, we observe a direct link between folding and metalation of the ALS-associated enzyme SOD1. Coordination of Zn^{2+} to the low-affinity Cu site occurs early in the folding reaction and stabilizes the critical folding nucleus, whereas coordination of Zn^{2+} to the high-affinity Zn site occurs late and selectively stabilizes the folded state. Accordingly, Zn^{2+} will first catalyze the SOD1 folding reaction by coordinating transiently to the Cu ligands and then, after the monomer is folded, transfer to the more stable position in the native Zn site

(43) Bosco, G. L.; Baxa, M.; Sosnick, T. R. *Biochemistry* **2009**, *48* (13), 2950–2959.
(44) Krantz, B. A.; Sosnick, T. R. *Nat. Struct. Biol.* **2001**, *8* (12), 1042–1047.
(45) Maret, W. *Biometals* **2009**, *22* (1), 149–157.
(46) Lamb, A. L.; Torres, A. S.; O'Halloran, T. V.; Rosenzweig, A. C. *Nat. Struct. Biol.* **2001**, *8* (9), 751–755.
(47) Furukawa, Y.; O'Halloran, T. V. *Antioxid Redox Signaling* **2006**, *8* (5−6), 847–867.
(48) Leitch, J. M.; Yick, P. J.; Culotta, V. C. *J. Biol. Chem.* **2009**, *284* (37), 24679–24683.
(49) Assfalg, M.; Banci, L.; Bertini, I.; Turano, P.; Vasos, P. R. *J. Mol. Biol.* **2003**, *330* (1), 145–158.
(50) Banci, L.; Bertini, I.; Cramaro, F.; Del Conte, R.; Viezzoli, M. S. *Biochemistry* **2003**, *42* (32), 9543–9553.

(Figure 8). The latter step also increases the lifetime of the folded SOD1 monomer from hours to years, suggesting that degradation and turnover of SOD1 *in vivo* are controlled dynamically by demetalation. This ability of Zn^{2+} to alter so radically the lifetime of the folded SOD1 molecule brings forward the Zn^{2+} coordination dynamics as critical modulator of misfolding and gain of toxic function in ALS.

Materials and Methods

SOD1 Mutants Analyzed in This Study. $SOD1^{CuZn}$ (F50E/G51E/C6A/C111A): monomeric SOD1 containing all the metal binding ligands of the wild-type protein, constructed by the dimer-splitting mutations F50E/G51E[13] and prevented from erroneous disulfide cross-linking by the mutations C6A/C111A.[12] **$SOD1^{XZn}$** (F50E/G51E/C6A/C111A/H46S/H48S/H120S): monomeric SOD1 without the Cu binding ligands H46, H48, and H120, constructed on a background of $SOD1^{CuZn}$. **$SOD1^{CuX}$** (F50E/G51E/C6A/C111A/H63S/H71S/H80S/D83S):[3] monomeric SOD1 without the Zn binding ligands H63, H71, H80, and D83, constructed on a background of $SOD1^{CuZn}$.

Protein Preparation. The proteins $SOD1^{CuZn}$, $SOD1^{XZn}$, and $SOD1^{CuX}$ were coexpressed with the copper chaperone yCCS and purified as described in ref 51. The procedure yields metalated holo species ("as-purified") with predominantly Cu-loaded Cu site (not applicable for $SOD1^{XZn}$) and Zn^{2+}-loaded Zn site. Apo protein was prepared as in ref 52 using 10 mM bis-Tris (SIGMA) at pH 6.3. To obtain $SOD1^{XZn}$ species with fractional Zn^{2+} loading of the Zn site or $SOD1^{CuZn}$ with Zn^{2+} in both Cu and Zn sites, folded apo protein was incubated with $ZnCl_2$ in 10 mM bis-Tris at pH 6.3. For high concentrations of $ZnCl_2$ (500 μM), the incubation time was 1 h, and for low concentrations of $ZnCl_2$ (<500 μM), it varied between 24 and 96 h. For 1:1 protein/Zn^{2+} ratios, we also used as-purified protein that had not been subject to apo treatment and in vitro metalation.

Crystallization. Crystals of holo$SOD1^{CuZn}$ and holo$SOD1^{XZn}$ were grown in 5−7 days by the hanging-drop vapor-diffusion method at room temperature. The crystallization drops for holo$SOD1^{CuZn}$ were made by mixing 1 μL of protein (10 mg/mL in H_2O) with 1 μL of reservoir solution containing 25% PEG 6000, 0.1 M MES pH 6.0, 0.01 M $ZnCl_2$. Holo$SOD1^{XZn}$ crystals were grown using drops consisting of 1 μL of protein (10 mg/mL in H_2O) and 1 μL of a reservoir solution containing 25% PEG 6000, 0.1 M sodium acetate pH 5.0, 0.01 M $ZnCl_2$.

Data Collection and Refinement. Protein crystals were cryoprotected by rapid soaking in a mother liquor supplemented with 25% (v/v) glycerol, before flash-cooling in a stream of gaseous N_2 at 100 K. X-ray diffraction data were collected at 100 K on a marResearch CCD detector at wavelength of 0.9085 Å on the I911-5 beamline of the MAX-lab synchrotron, Lund, Sweden. All images were processed, data scaled, and merged using XDS.[53] Data collection statistics are given in Table 1. The holo$SOD1^{CuZn}$ structure was solved by the molecular replacement program Phaser[12] using monomeric holoSOD1(F50E/G51E/E133Q), PDB entry 1MFM[13] as a starting model. The holo$SOD1^{XZn}$ structure was solved with standard rigid body refinement using Refmac5,[54] as implemented in CCP4 suite,[11] with the holo$SOD1^{CuZn}$ structure as a starting model after removal of the Cu atom. The structures were refined using Refmac5, with the maximum likelihood target function and using anisotropic B factors. Five percent of the total reflections were flagged randomly for cross-validation before refinement. TLS parametrization was used in the latter stage of refinement, with one set of parameters for the entire molecule.[55] For further details, see Supporting Information. Structures were visualized and modified using Coot,[14] and the stereochemistry of the models was evaluated with PROCHECK.[56] Refinement and geometrical statistics are summarized in Table 1. Structural alignments were made with the SSM algorithm[57] as implemented in Coot and figures made with PyMOL (www.pymol.org). Atomic coordinates and structure factors have been deposited in the RCSB Protein Data Bank as entry 2XJK for holo$SOD1^{CuZn}$ and 2XJL for holo$SOD1^{XZn}$.

Folding and Unfolding Experiments. Folding and unfolding experiments were conducted at 25 °C in 10 mM bis-Tris at pH 6.3, with urea (ultra PURE, MP Biomedicals, Inc.) as denaturant. The protein concentration in the detection volume was in all cases 5 μM of monomer. Equilibrium unfolding and slow kinetics ($\log k_{obs} < -2.5$) were measured on a Varian Cary Eclipse spectrophotometer (Varian Inc., USA) with excitation at 280 nm and collected emission at 335−375 and 360 nm, respectively. Fast kinetics ($\log k_{obs} > -2.5$) was followed on a SX-18MV stopped-flow device (Applied Photophysics, Leatherhead, UK) with excitation at 280 nm and emission collected above 305 nm with a cutoff filter.

Metal-Release Measurements. Kinetics of Zn^{2+} release was measured by unfolding of 5 μM Zn^{2+}-coordinated protein in the presence of 500 μM EDTA (SIGMA) or the fluorescent chelator ZINPYR-1 (SIGMA). In the latter case, the protein and ZINPYR-1 concentrations in the detection volume were 1.3 and 2.6 μM, respectively, with excitation at 490 nm and detection at 527 nm using a band-pass filter.

Data Analysis. The SOD1 monomers were assumed to display two-state behavior in apo form and holo forms, yielding the expression

$$K_{U/F} = [U]/[F] = k_u/k_f \tag{8}$$

where U and F are the unfolded and folded monomers, respectively, and k_u and k_f are the unfolding and refolding rate constants, respectively.[12,22,58] Protein stability, $\Delta G_{U/F} = -2.3RT\log K_{U/F}$, was further assumed to depend linearly on [urea] yielding

$$\begin{aligned} &\log K_{U/F} = \log K^0 + m_{U/F}[\text{urea}] \text{ and} \\ &\log k_f = \log k_f^0 + m_f[\text{urea}] \\ &\log k_u = \log k_u^0 + m_u[\text{urea}] \end{aligned} \tag{9}$$

Accordingly, the transition midpoint (MP) and $m_{U/F}$ were derived from equilibrium data (Figure 3)

$$F_{obs} = (a + b10^{m_{U/F}([\text{urea}]-MP)})/(1+10^{m_{U/F}([\text{urea}]-MP)}) \tag{10}$$

where F_{obs} is the measured fluorescence, and a and b are sloping base lines.[58] The kinetic data (Figures 3 and 4) were fitted to the standard two-state expression[12]

$$\log k_{obs} = \log(10^{\log k_f^{H_2O} + m_f[\text{urea}]} + 10^{\log k_u^{H_2O} + m_u[\text{urea}]}) \tag{11}$$

(51) Lindberg, M. J.; Tibell, L.; Oliveberg, M. *Proc. Natl. Acad. Sci. U.S.A.* **2002**, *99* (26), 16607–16612.
(52) Lindberg, M. J.; Bystrom, R.; Boknas, N.; Andersen, P. M.; Oliveberg, M. *Proc. Natl. Acad. Sci. U.S.A.* **2005**, *102* (28), 9754–9759.
(53) Kabsch, W. *J. Appl. Crystallogr.* **1993**, *26* (6), 795–800.
(54) Murshudov, G. N.; Vagin, A. A.; Dodson, E. J. *Acta Crystallogr. D* **1997**, *53* (Pt 3), 240–255.
(55) Winn, M. D.; Isupov, M. N.; Murshudov, G. N. *Acta Crystallogr. D* **2001**, *57* (Pt 1), 122–133.
(56) Laskowski, R. A.; MacArthur, M. W.; Moss, D. S.; Thornton, J. M. *J. Appl. Crystallogr.* **1993**, *26* (2), 283–291.
(57) Krissinel, E.; Henrick, K. *Acta Crystallogr. D* **2004**, *60* (Pt 12, Pt 1), 2256–2268.
(58) Fersht, A. R. *Structure and Mechanism in Protein Science: A Guide to Enzyme Catalysis and Protein Folding*; WH Freeman and Co.: New York, 1999.

where $k_f^{H_2O}$ and $k_u^{H_2O}$ are the rate constants at 0 M urea, and m_f and m_u the slopes of the refolding and unfolding limbs, respectively. The software for data analysis was Kalaidagraph.

Acknowledgment. We wish to thank Stefan Marklund for valuable discussions, Maria Håkansson for help at the MAX-lab macromolecular crystallization facility, as well as staff at the MAX-lab beamline I911 for assistance with data collection. This work was financed by grants from Swedish Research Council, the Knut and Alice Wallenberg Foundation, the Bertil Hållsten Foundation and Hjärnfonden to M.O. and from the Swedish Research Council to D.T.L.

Supporting Information Available: Anisotropy of Cu^{2+} in the crystal structure of monomeric holoSOD1^{CuZn}; alternate conformations of loop IV in the crystal structure of monomeric holoSOD1^{CuZn}; deviation from first-order unfolding kinetics of holoSOD1^{XZn} at low concentrations of solvent Zn^{2+}; crystal structure refinement; and complete ref 25. This material is available free of charge via the Internet at http://pubs.acs.org.

JA1057136